Pergamon

0967-0637(94)00042-5

Deep-Sea Research I, Vol. 42, No. 2, pp. 165–189, 1995

0967–0637/95 $9.50 + 0.00

On the synoptic hydrography of intermediate and deep water masses in the Iceland Basin

H. M. VAN AKEN* and C. J. DE BOER*

(*Received* 26 *March* 1993; *in revised form* 9 *February* 1994; *accepted* 25 *April* 1994)

Abstract—The hydrography of intermediate and deep water masses in the Iceland Basin is studied from quasi-synoptic surveys carried out in 1990 and 1991. The general water mass structure was identical for both years. The interaction and mixing of the different water types present in the basin is reviewed by means of property–property plots, vertical tracer sections and isopycnal analyses. It appears that overflow waters from the Norwegian Sea are modified in successive stages during their descent into the deep Iceland Basin. They mix with Sub-Polar Mode Water at short distances from the sills in the Faroe Bank Channel and on the Iceland–Faroe Ridge, thereby forming Iceland–Scotland Overflow Water. This water type entrains Labrador Sea water during the descent into the deep Iceland Basin, where Iceland–Scotland Overflow Water is further modified mainly by diapycnal mixing with overlying Lower Deep Water, which contains a large fraction of Antarctic Bottom Water. At intermediate levels Labrador Sea Water and Intermediate Water appear to mix laterally with a slope water mass flowing along the Icelandic and Reykjanes slopes. This slope water is formed by the direct mixing of Iceland–Scotland Overflow Water with Sub-Polar Mode Water and differs from the water mass, encountered in the central Iceland Basin. The intermediate and deep circulation in the Iceland Basin has a cyclonic character with smaller-scale variations due to topographic steering along ridges on the Icelandic slope.

1. INTRODUCTION

THE Iceland Basin in the northern northeast Atlantic is an important area for thermohaline oceanic heat transport. Through this area exchanges between the Atlantic Ocean and the Arctic and Polar seas take place. Warm and salty Atlantic water originating from the Gulf Stream enters the Norwegian Sea in the upper layers west as well as east of the Faroes. In the Nordic Seas and the Polar Ocean this water is modified by cooling and freezing to a number of distinctive Polar and Arctic water types (SWIFT and AAGAARD, 1981; RUDELS and QUADFASEL, 1991) which flow back into the Atlantic Ocean. Part of this return flow takes place at deeper levels by overflow through the Faroe Bank Channel and across the Iceland–Faroe Ridge into the Iceland Basin (DOOLEY and MEINCKE, 1981; VAN AKEN and EISMA, 1987). Another main path for the return flow is the overflow through the Denmark Strait into the Irminger Basin (e.g. DICKSON *et al.*, 1990), while minor overflow is observed across the Wyville Thomson Ridge into the Rockall Trough (ELLETT and ROBERTS, 1973).

Because of diapycnal mixing during the overflow across the Faroe Bank Channel and the Iceland–Faroe Ridge, the properties of the different Arctic and Polar water types change, and a new more or less homogeneous original water type is formed (VAN AKEN and

*Netherlands Institute for Sea Research, P.O. Box 59, 1790AB Den Burg, the Netherlands.

EISMA, 1987) for which we will use the name Iceland–Scotland Overflow Water (ELLETT and MARTIN, 1973). In the Iceland Basin, downstream from the overflow sills, further modification may take place by mixing with other water types present in the Iceland Basin, e.g. Labrador Sea Water and Lower Deep Water (MCCARTNEY, 1992) or Mediterranean Overflow Water (HARVEY and THEODOROU, 1986). The resulting water type flows from the Iceland Basin through the Charlie-Gibbs Fracture Zone into the western North Atlantic, where it is one of the main constituents for the formation of the North Atlantic deep-water complex (BROECKER and TAKAHASHI, 1980; MCCARTNEY, 1992).

Most studies on the deep circulation and mixing in the Iceland Basin are based on compilations of hydrographic data from different cruises and different years (TALLEY and MCCARTNEY, 1982; MCCARTNEY and TALLEY, 1982; HARVEY and THEODOROU, 1986; TSUCHIYA, 1989; MCCARTNEY, 1992). Such an approach may encounter difficulties, because the properties of the original Arctic and Polar water types which participate in the overflow may vary inter-annually (DOOLEY *et al.*, 1984), while the properties of the Atlantic water types also vary on inter-annual time scales (TALLEY and MCCARTNEY, 1982; BREWER *et al.*, 1983; READ and GOULD, 1992).

In this paper we present results from synoptic hydrographic surveys of the Iceland Basin carried out in 1990 and 1991 as part of the DUTCH-WARP programme. From the distributions and mutual relations among hydrographic parameters we discuss how the different intermediate and deep water types in the Iceland Basin interact and are modified, with emphasis on the overflow water originating from the Norwegian Sea. The discussion will be based mainly on the 1991 data. Additional results from long term current meter moorings are also used. The current meter data are discussed in more detail by VAN AKEN (1993).

No geostrophic transports are discussed in this paper since no clear level of no motion can be derived from the observations. Transport estimates based on inverse modelling will be presented in a separate paper, and the temporal hydrographic and current variations will also be presented separately.

2. OBSERVATIONS AND DATA PROCESSING

In July 1990 and in April/May 1991 R.V. *Tyro* carried out hydrographic surveys in the northern Atlantic (Fig. 1). These surveys consisted of the WOCE Hydrographic Programme repeat section AR7 (eastern part) from the Irish continental shelf to Greenland (station spacing 30 n. miles) and a number of high-resolution hydrographic sections (station spacing 15 n. miles) in the northern Iceland Basin. In 1990 the AR7 section went around the Rockall Hatton Plateau towards the Reykjanes Ridge at 59°N, while in 1991 this section had a more zonal orientation at a nominal latitude of 58°N (Fig. 1). High-resolution sections A, B, C, E and F were surveyed in 1990. These sections were repeated in 1991 and additional sections G, H and I near the Iceland–Faroe Ridge and section J from Lousy Bank to Hatton Bank were surveyed.

A CTD down-cast was recorded at each station, and during the up-cast water samples were taken for the analysis of salinity, nutrients and oxygen. On the first, third and fifth Niskin bottle electronic reversing thermometers were mounted (resolution and accuracy 1 mK) together with an electronic reversing pressure sensor (resolution 1 dbar, accuracy 1.5 dbar). The data obtained during the up-cast were used for calibration.

The raw CTD-data recorded during the down-cast were despiked and averaged over

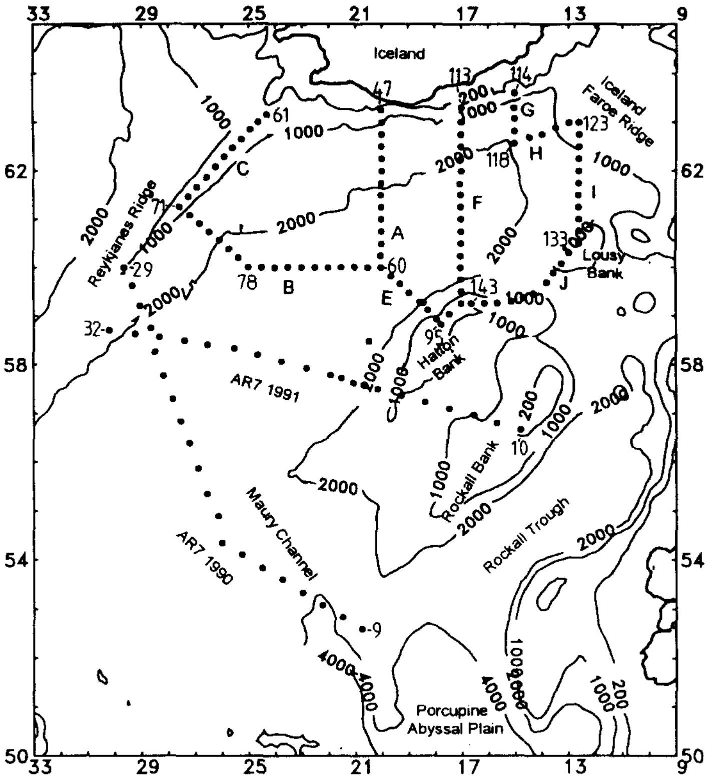

Fig. 1. Topography of the Iceland Basin with the hydrographic stations used in this paper. The Iceland Basin is situated between the Rockall–Hatton Plateau and the Reykjanes Ridge. The southern deep entrance of the Iceland Basin is in the Maury Channel with depth over 4000 m. The shallow ridge, south-east of eastern Iceland is the Iceland–Faroe Ridge. The southernmost AR7 section and sections A, B, C, D, E and F were surveyed in 1990, Sections A, B, C, E and F were repeated and the northern AR7 section and sections G, H, I and J were surveyed in 1991. Stations along AR7 in the Rockall Trough and in the Irminger Sea are not shown.

0.6 s time bins, with a correction for the response time mismatch of the sensors. These time bins correspond to pressure bins of about 1 dbar, given the typical lowering velocity of 1.5 m s^{-1}. The time-averages were interpolated on uniformly increasing 1 dbar pressure levels. The estimated accuracy (RMS values) of the calibrated CTD parameters are better than 2.5 dbar for pressure, 1.7 mK for temperature, and 0.0017 for practical salinity (van Aken, 1990, 1992). The potential temperature Θ is calculated according to the International Temperature Scale 1990 (ITS-90), the salinity S according to the Practical Salinity Scale 1978 (PSS-78), and the density according to the International Equation of State of sea water 1980 (EOS-80) (JPOTS editorial panel, 1991). The potential density anomaly is depicted by σ_n, where the subscript n refers to the reference pressure ($n \cdot 1000$ dbar). We will use the pressure in dbar as vertical co-ordinate.

The oxygen concentrations (O_2) were determined by means of an automated Winkler titration with a high-precision photometric end point determination and were corrected for the values of the sample blanks. The accuracy of the O_2 values is estimated to be better than 0.5 μmol kg^{-1}. The concentrations of the nutrients dissolved silica (Si) and nitrate

Table 1. Positions of the long term current meter moorings in the Iceland Basin

Mooring	Latitude	Longitude	Water depth
IB89/1	61°33.1′N	20°00.8′W	2120 m
IB90/1	61°34.1′N	19°57.8′W	2118 m
IB90/2	60°59.6′N	19°59.3′W	2388 m
IB90/3	59°16.1′N	18°24.7′W	1906 m

Table 2. Averages and standard deviations from long term current meter moorings in the Iceland Basin

Mooring	Depth C.M. (m)	East component mean (cm s^{-1})	East component S.D. (cm s^{-1})	North component mean (cm s^{-1})	North component S.D. (cm s^{-1})	Temperature mean (°C)	Temperature S.D. (°C)	Period start–end
IB89/1	1320	−1.2	7.8	1.6	7.2	3.70	0.07	Aug.89–Dec.89
IB89/1	1520	−2.3	7.9	0.7	7.7	3.52	0.06	Aug.89–Dec.89
IB89/1	1920	−12.8	7.4	1.4	5.7	3.08	0.15	Aug.89–Dec.89
IB90/1	1318	−3.2	13.8	2.1	9.9	3.89	0.08	Jul.90–Aug.90
IB90/1	1518	−3.9	9.0	1.0	8.3	3.49	0.07	Jul.90–Dec.90
IB90/1	1918	−15.2	7.8	−1.5	3.1	2.98	0.32	Jul.90–Jan.91
IB90/1	2078	−17.7	8.0	−7.2	5.0	2.53	0.25	Jul.90–Feb.91
IB90/2	1388	6.2	8.0	1.7	11.2	3.81	0.13	Jul.90–Jan.91
IB90/2	2188	4.6	6.6	−2.9	7.7	2.91	0.20	Jul.90–Jan.91
IB90/2	2348	3.1	6.3	−4.7	6.4	2.26	0.14	Jul.90–Feb.91
IB90/3	1006	−0.4	3.7	1.4	3.2	5.16	0.39	Jul.90–Jan.91
IB90/3	1706	2.4	4.6	2.2	3.9	3.59	0.03	Jul.90–Feb.91
IB90/3	1867	3.9	4.8	3.0	4.7	3.48	0.07	Jul.90–Jan.91

(NO_3) were measured with a TRAACS auto-analyser. Their respective accuracies are 0.07 μmol kg^{-1}, and 0.1 μmol kg^{-1} (van Aken, 1990, 1992). The oxygen and nutrient values were inspected and occasional outliers were rejected.

From the temperature and salinity profiles the (planetary) potential vorticity, λ, was estimated as:

$$\lambda = \frac{f \cdot N^2}{g} \tag{1}$$

(McDowell *et al.*, 1982), where f is the Coriolis frequency, N is the Brunt–Väisälä frequency and g is the gravitational acceleration. For the computation of λ a central finite difference over a pressure interval of 100 dbar was used.

Some results from long term current measurements in the Iceland Basin, carried out in 1989–1990 and 1990–1991 are used in this paper (Table 1). The results of these measurements have been compiled in van Aken and Ober (1991, 1992). Mean values and standard deviations of the east and north components of the current and of the water temperature are given in Table 2. These values have been derived from low pass filtered data in which variations with diurnal and higher frequencies are suppressed.

For the isopycnal analyses presented in this paper the bottle data and CTD data were first interpolated vertically on the required density surface. In order to prevent aliasing of small scale variability of the tracers in the along-section direction to larger scales in the direction perpendicular to the hydrographic sections, the interpolated data were then smoothed in the along-section direction by the application of a three station running average.

3. THE WATER MASSES OF THE ICELAND BASIN

3.1. *The water mass structure*

A compilation of the hydrographic data is given as plots of S, O_2, Si and NO_3 versus Θ (Fig. 2). All bottle data from 1991 have been used as well as the AR7 data from 1990 in order to maximize the geographic coverage of the Iceland Basin without duplicating the repeat sections. These plots reveal the characteristic relations typical of the water mass structure of the Iceland Basin.

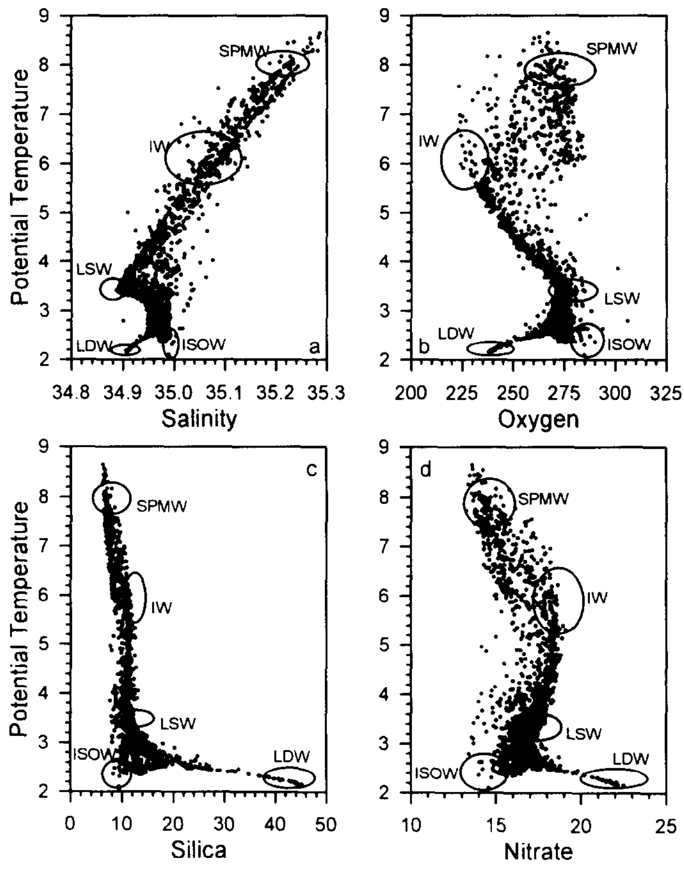

Fig. 2. Plots of Θ (°C) versus S (a), O_2 (μmol kg^{-1}), (b), Si (μmol kg^{-1}) (c) and NO_3 (μmol kg^{-1}) (d). These plots are based on water samples taken below 500 dbar at all stations occupied in 1991, combined with section AR7 from 1990. The location of the different water types discussed in this paper is indicated with ellipses identified by acronyms.

For the discussion of the water masses we will use in this paper the term water type in the sense of a considerable amount of water with a common formation history and a limited variation in its characteristic hydrographic parameters. The term water mass is used for a continuum of water, formed by the mixing of at least two water types. Hereby it is assumed that the within-type variance of the hydrographic parameters is definitely smaller than the between-type variance. The water types characteristic of the Iceland Basin are indicated with ellipses and acronyms in Fig. 2. The hypothetical, homogeneous sources from which these water types are assumed to be derived are named source water types, each characterized by a single vector in the hydrographic parameter space. These source water types are an idealization of the real water types.

Water types have been recognized from extremes in the property–property plots (Fig. 2). The near surface layer contains Sub-Polar Mode Water (SPMW), characterized by high temperatures and salinities. In the permanent thermocline O_2 minima and Si and NO_3 maxima are found, related to the biogeochemically defined Intermediate Water (IW), while below the permanent thermocline the salinity minimum related to the presence of Labrador Sea Water (LSW) can be observed. In the cold near bottom layers maxima of S and O_2 and minima of Si and NO_3 are connected with Iceland Scotland Overflow Water (ISOW), while the minima of S and O_2 and maxima of the nutrients are related to the presence of Lower Deep Water (LDW) of southern origin. In the following sections these water types will be discussed.

The relative amount of the different water types present in the northern Iceland Basin in both years can be seen from contour plots of $P(\Theta,S)$, the bivariate probability density of Θ and S (Fig. 3). Integration of $P(\Theta,S)$ over all possible Θ and S values will result in a probability of 1 to find any Θ–S value. This is a statistical variation of the volumetric water mass census (e.g. WORTHINGTON, 1981). This probability distribution has been calculated from CTD data at 1 dbar intervals for the repeat sections A, B, C, E and F of the station grid south of Iceland. For the estimate of $P(\Theta,S)$ a frequency count in 0.1°C Θ intervals and 0.01 S intervals was used. Comparison of the probability distributions for 1990 (Fig. 3a) and 1991 (Fig. 3b) shows only slight changes from year to year while the general probability structure is the same for both years. For 1990 water with $\Theta < 2.5$°C has a slightly higher probability than for 1991 with a smaller variability in S, indicating a larger amount of ISOW being present in 1990, compared with 1991. Analysis of the spatial distribution of the hydrographic parameters along the repeated sections (not shown here) has revealed that the spatial hydrographic structure was also quite similar for both years. Because of the large similarity in overall Θ–S structure and spatial structure for both years, we assume that we can combine data from both years in our analysis.

The spatial structure of the hydrographic fields is depicted in vertical sections of Θ, S, O_2 and Si along sections AR7 (1991) (Fig. 4), B and E (Fig. 5), and F (Fig. 6). The derived hydrographic parameter λ along section B and E is shown in Fig. 7. We will refer to Figs 2–7 in the following discussion of the individual water types.

3.2. *Sub-polar Mode Water*

The Θ–S plot for the Iceland Basin (Fig. 2a) shows the presence of SPMW with high Θ and S values formed by winter time convection (MCCARTNEY and TALLEY, 1982). The potential temperature of SPMW varied along section AR7 from 9 to 10°C in the Rockall Trough to about 6°C over the Reykjanes Ridge and 3–3.5°C in the centre of the Irminger

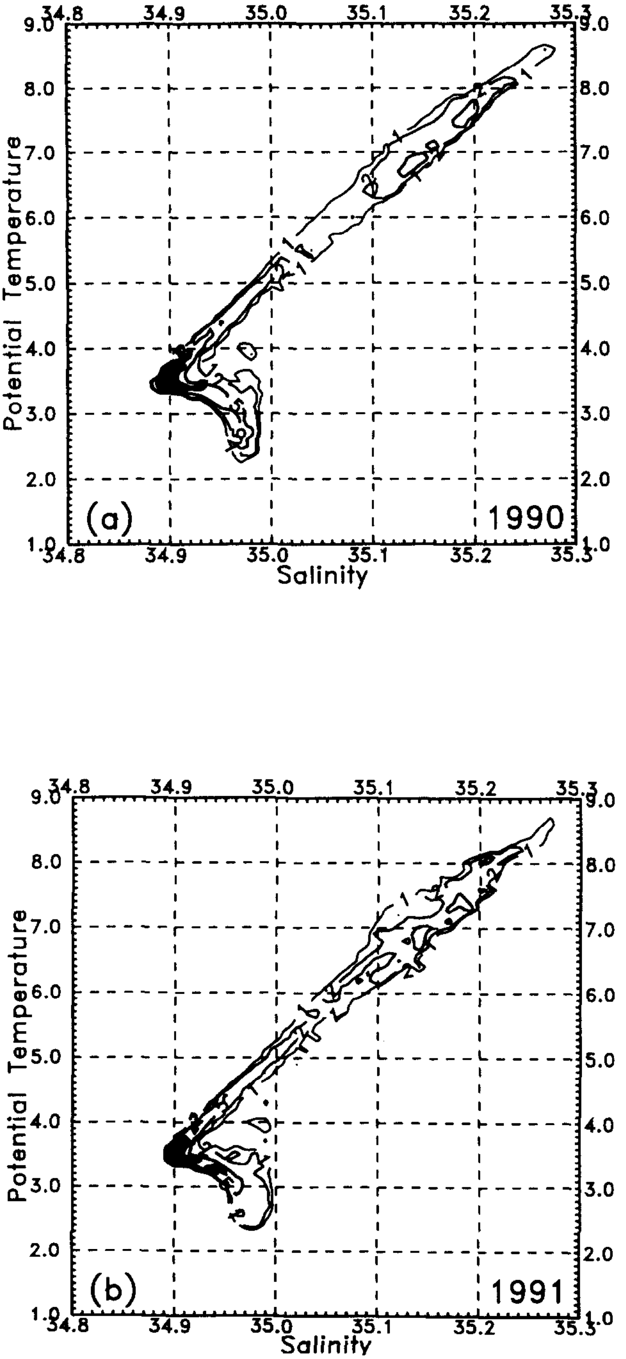

Fig. 3. The bivariate probability density $P(\Theta, S)$ ($°C^{-1}$) for sections A, B, C, E and F in 1990 (a) and 1991 (b). Frequency of observations at dbar intervals: for the estimate of $P(\Theta, S)$ a frequency count in 0.1°C temperature intervals and 0.01 salinity intervals was used. The blackened area indicates the $P > 10°C^{-1}$ region.

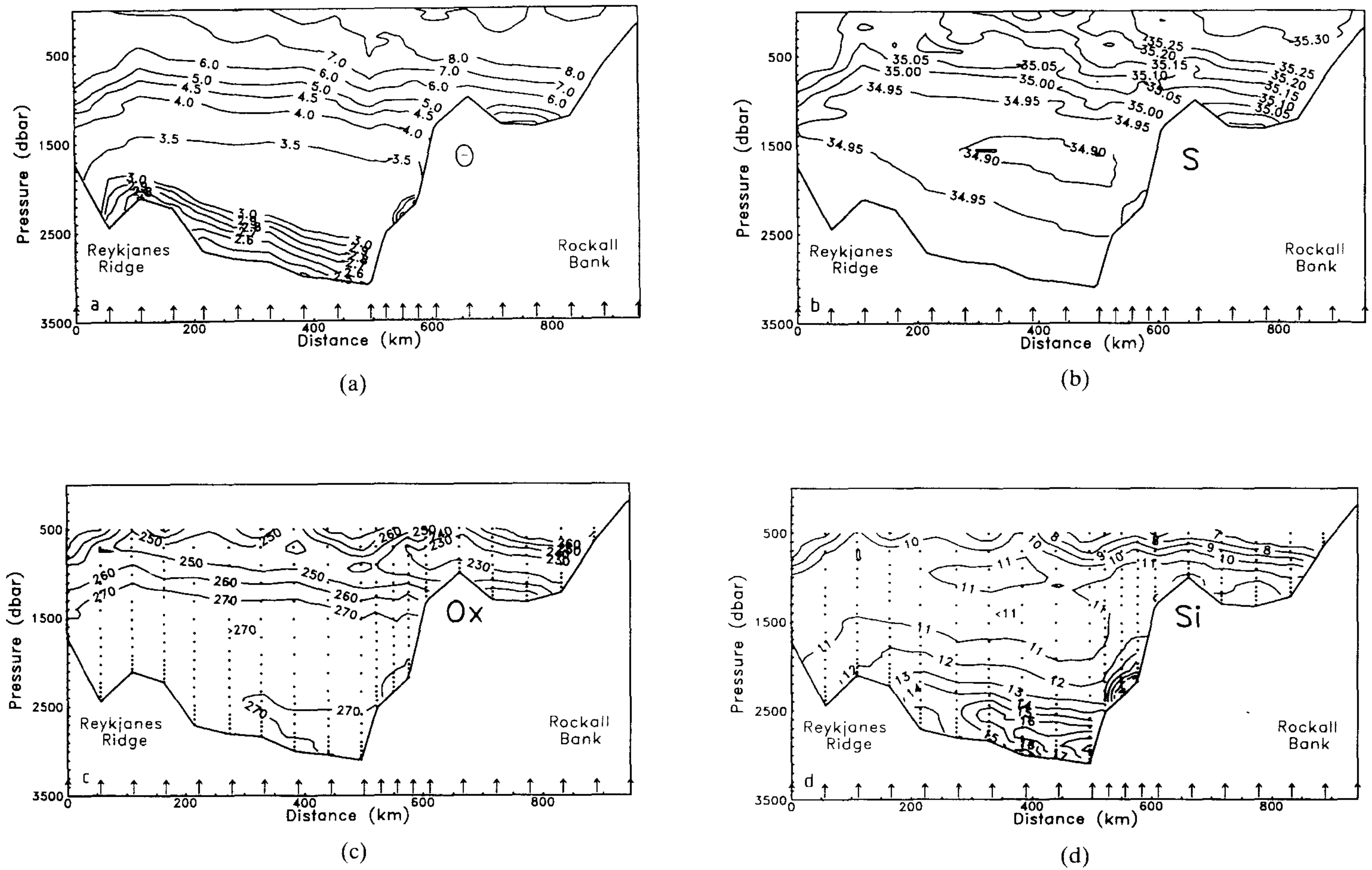

Fig. 4. Vertical sections of (a) Θ (°C), (b) S, (c) O_2 (μmol kg^{-1}) and (d) Si (μmol kg^{-1}) for the 1991 AR7 section at about 58°N in the Iceland Basin. The arrows indicate the position of the hydrographic stations on this section.

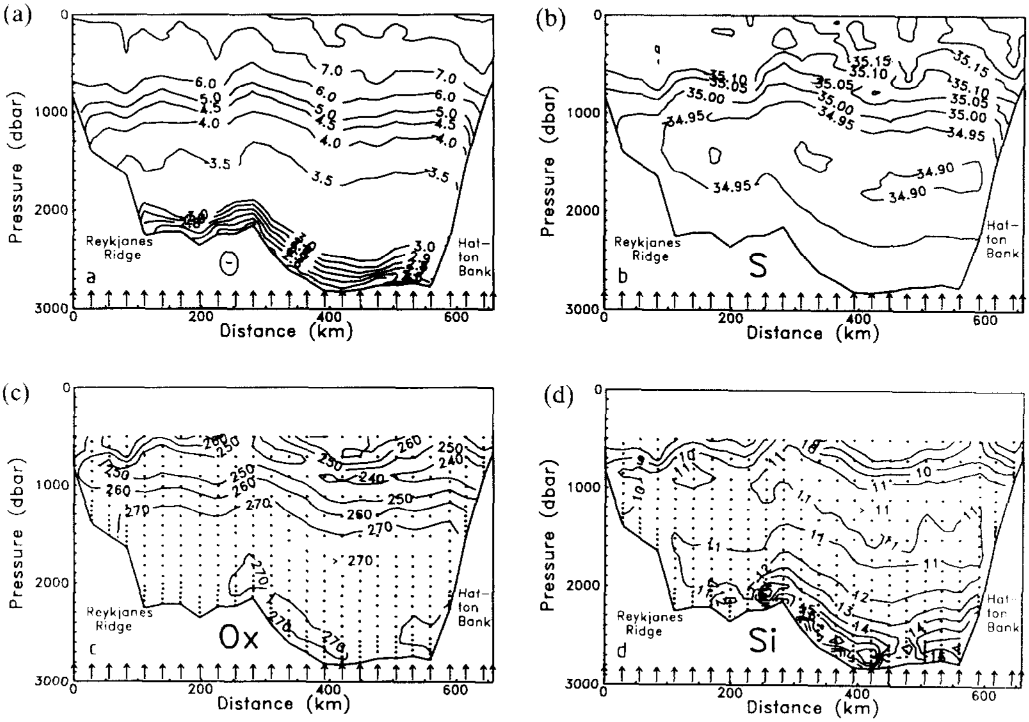

Fig. 5. As Fig. 4 for the 1991 combined B and E sections at about 60°N.

Sea (VAN AKEN, 1990, 1992). Also along the sections A–F within in the northern Iceland Basin the Θ–S properties of SPMW show a range of values (Figs 4–6). SPMW has high O_2 values compared with the underlying colder water (Fig. 2b) and low nutrient concentrations (Fig. 2c, d). Since this water type is convectively formed, SPMW can be recognized from a λ minimum below the seasonal thermocline (Figs 5a and 7). SPMW can interact directly with the deep water types entering the Iceland Basin only where they are in direct contact, that is near the shallow sills in the Faroe Bank Channel and over the Iceland–Faroe Ridge (VAN AKEN and EISMA, 1987). There SPMW was characterized by $\Theta \approx 8.00°C$, $S \approx 35.230$, and $Si \approx 6.3\,\mu mol\ kg^{-1}$, in agreement with MCCARTNEY and TALLEY (1982).

3.3. *Intermediate Water*

In the permanent thermocline of the Iceland Basin, minima of O_2 and maxima of NO_3 (Fig. 2b, d) at $\Theta \approx 6°C$ reveal the presence of biogeochemically defined IW which has no specific signature in the Θ–S space (Fig. 2a). In Fig. 2c maxima of Si connected with IW can hardly be discerned, but the vertical Si sections (Figs 3d, 4d and 5d) show the presence of maxima in $Si > 11\,\mu mol\ kg^{-1}$, nearly coinciding with the extremes in O_2 (Figs 3c, 4c and 5c) and NO_3. The origin of IW in the Iceland Basin may be either aged Antarctic Intermediate Water, brought there with the Gulf Stream and the North Atlantic current (MANN *et al.*, 1973; BROECKER and TAKAHASHI, 1981; TSUCHIYA, 1989) or "Africa Water" transported northward along the African and European shelf "coastally trapped" in an eastern

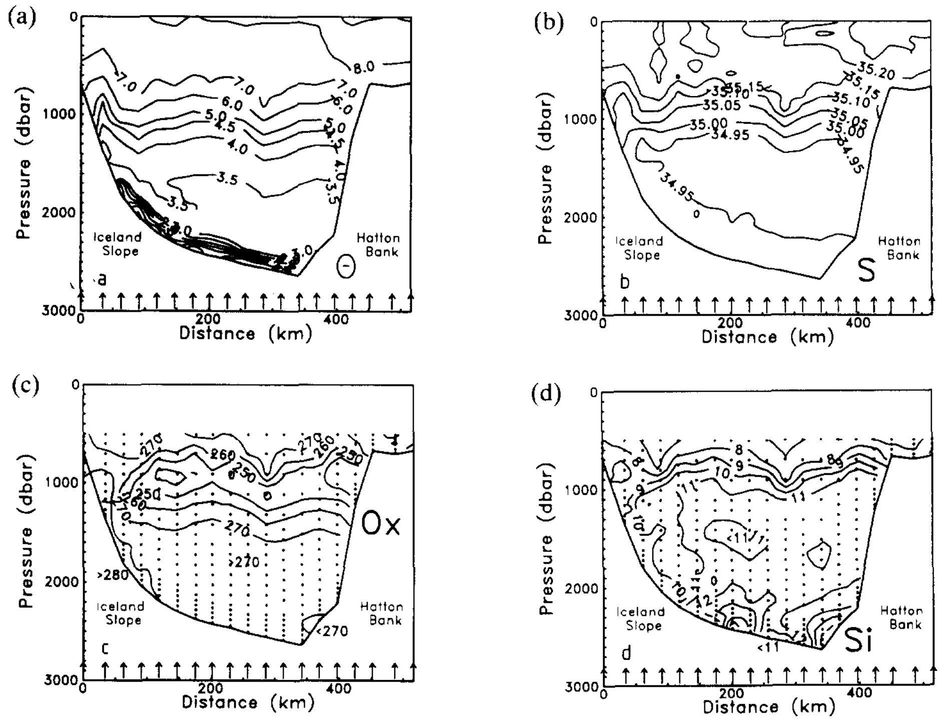

Fig. 6. As Fig 4 for the 1991 meridional section F at 17°W.

boundary current (Kawase and Sarmiento, 1986). The presence of near bottom Si maxima in the shallow basin between the Rockall Bank and the Hatton Bank (Fig. 4d) below the O_2 minima (Fig. 4c) indicates the importance for IW properties of regeneration of Si over the Rockall–Hatton Plateau due to sediment–water interaction. De Boer (1993) ascribes the biogeochemical properties of IW mainly to regeneration of organic matter. From the O_2 and Si section in the Northern Iceland Basin (Figs 5c, d and 6c, d), it appears that at the levels where IW is found over the Icelandic and Reykjanes slopes, water with relatively high O_2 and low Si concentrations is found. Near the overflow cores over the Iceland–Faroe Ridge, IW was virtually absent and is therefore assumed not to contribute significantly to the modification of ISOW.

3.4. *Labrador Sea Water*

LSW is characterized by S minima below 34.90 (Fig. 2a) and O_2 maxima above 275 μmol kg^{-1} (Fig. 2b). LSW is formed by the final modification of SPMW in the Labrador Sea (Talley and McCartney, 1982) and contributes to the formation and modification of various types of North Atlantic deep waters (Lee and Ellett, 1967; Harvey and Theodorou, 1986; Kawase and Sarmiento, 1986; McCartney, 1992). The Θ–S properties of LSW present the most frequently encountered water type in the Iceland Basin (Fig. 3) which is found at depth levels between 1300 and 2000 dbar (Figs 4–6). Along the Icelandic and Reykjanes slopes the salinity in this depth interval is systematically higher than in the centre of the Iceland Basin (Figs 4b, 5b and 6b). Because of its convective formation LSW

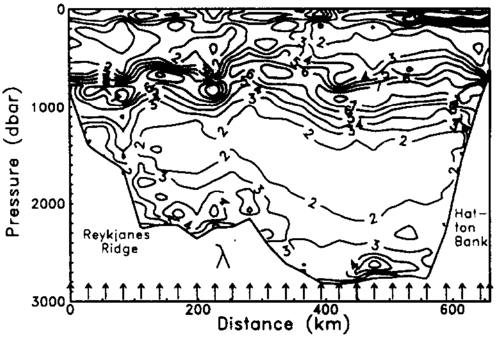

Fig. 7. Vertical section of potential vorticity (10^{-11} m^{-1} s^{-1}) for the combined 1991 B and E sections at about 60°N.

is also characterized by λ minima $< 2 \times 10^{-11}$ m^{-1} s^{-1} (TALLEY and MCCARTNEY, 1982) which coincide with the salinity minima (compare Figs 5b and 7). By extrapolation of the mixing lines towards LSW the local LSW source water type properties in the Iceland Basin were estimated to be $\Theta \approx 3.40$°C, S $\approx$ 34.885, Si $\approx$ 10.5 μmol kg^{-1}.

Along AR7 the Θ–S properties of the core of LSW in the Iceland Basin were intermediate between those of the neighbouring Irminger Sea and Rockall Trough (Fig. 8a). The S minima in the Iceland Basin and the Rockall Trough were found at the potential density level with $\sigma_{1.5}$ = 34.64 kg m^{-3}, while in the Irminger Sea the LSW core is found at $\sigma_{1.5}$ = 34.67 kg m^{-3}. Also the O_2 and Si values of the LSW core in the Iceland Basin differed from those in the neighbouring basins, the values in the Iceland Basin being intermediate between those of the Irminger Sea and the Rockall Trough (Fig. 8b, c). According to the property–property plots in Fig. 8 the observed increases of Θ, S and Si and the decrease of O_2 in the LSW core from the Irminger Sea via the Iceland Basin to the Rockall Trough may be explained from diapycnal mixing with the underlying and overlying water masses. Then it can be expected that the longest advection path from the Labrador Sea, that is to the Rockall Trough, will generate the strongest modification of LSW and the shortest path to the Irminger Sea the smallest modification, while the Iceland Basin is in an intermediate position. Such a geographical variation of S was also described by TALLEY and MCCARTNEY (1982, their Fig. 4) for observations from the late fifties and early sixties, only with overall slightly higher (0.03–0.05) salinities. This implies that diapycnal mixing probably plays a more important role than emphasized by READ and GOULD (1992), who ascribe the geographical differences in LSW properties observed in 1992 mainly to the advective propagation of temporal variations of the formation of LSW. However, with the available data the relative importance of diapycnal mixing and advection of temporally varying LSW for the observed geographic distribution cannot be established quantitatively.

The lateral distribution of S and λ at the $\sigma_{1.5}$ = 34.64 level (Fig. 9) shows that the distributions of these parameters are well correlated and agree with the large scale lateral non-synoptic distributions described by TALLEY and MCCARTNEY (1982). LSW is laterally bounded on its northern and western side by a water mass over the Icelandic and Reykjanes slopes characterized by a high salinity and potential vorticity (Figs 4, 7 and 9). This Icelandic slope water mass appears to originate from the Iceland–Faroe Ridge and the Faroe Bank Channel and to be advected westwards along the slope. The down-stream

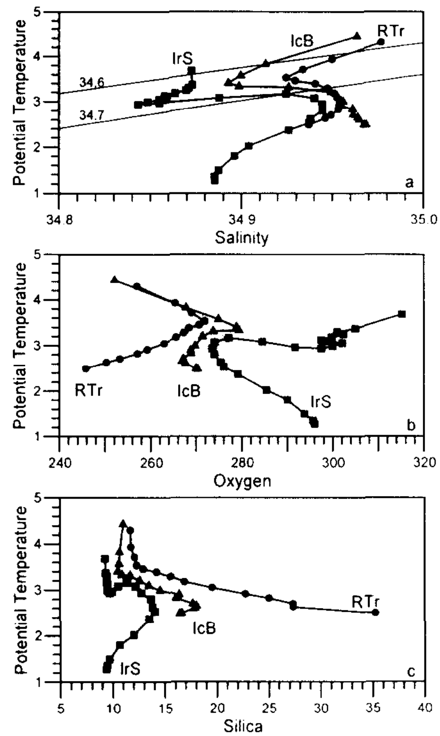

Fig. 8. Property–property plots of Θ (°C) versus (a) S, (b) O_2 (μmol kg^{-1}) and (c) Si (μmol kg^{-1}) for Sta. 6 in the Rockall Trough (56°18′N, 12°19′W, circles), Sta. 23 in the central Iceland Basin (57°56′N, 22°48′W, triangles) and Sta. 41 in the central Irminger Sea (59°29′N, 37°49′W, squares) from the 1991 AR7 section. In (a) the appropriate $\sigma_{1.5}$ lines are shown.

modification of this water mass is probably due to the isopycnal mixing with the LSW. Also along the edge of the Hatton Bank water with a slightly higher salinity and potential vorticity is observed (Fig. 9). Advection of the more modified LSW from the Rockall Trough in a deep northern boundary current along the slopes of the Rockall–Hatton Plateau (McCartney, 1992) can be ruled out as the cause of this anomalous LSW along the Hatton slope, since this would result in definitively higher Si concentrations (2–4 μmol kg^{-1}) than found along the Hatton slope (van Aken, 1992). Since the observed Θ–S properties do not show any evidence for the presence of Mediterranean Water in the Iceland Basin (Figs 2a and 3), we assume that this saltier water is formed by modification of LSW due to diapycnal boundary mixing while flowing north along the Hatton slope.

On all four moorings from Table 1 current meters were mounted at depths where LSW was found. The mean current vectors from these instruments (Table 2) are depicted in Fig. 9. The northward flow of the modified LSW is confirmed by current meter observations on section E near the 1900 m isobath (mooring IB90/3) which give a seven months mean north-eastward flow of 3.3 cm s^{-1} and a mean temperature of 3.59°C at a depth of 1706 m, close to the $\sigma_{1.5}$ = 34.64 kg m^{-3} isopycnal surface. The main inflow of the LSW core into the N.E. Iceland Basin appears to occur away from the topographic boundaries, since at 61°N, 20°W (IB90/2), at a depth of 1390 m, slightly above the LSW core, the seven months

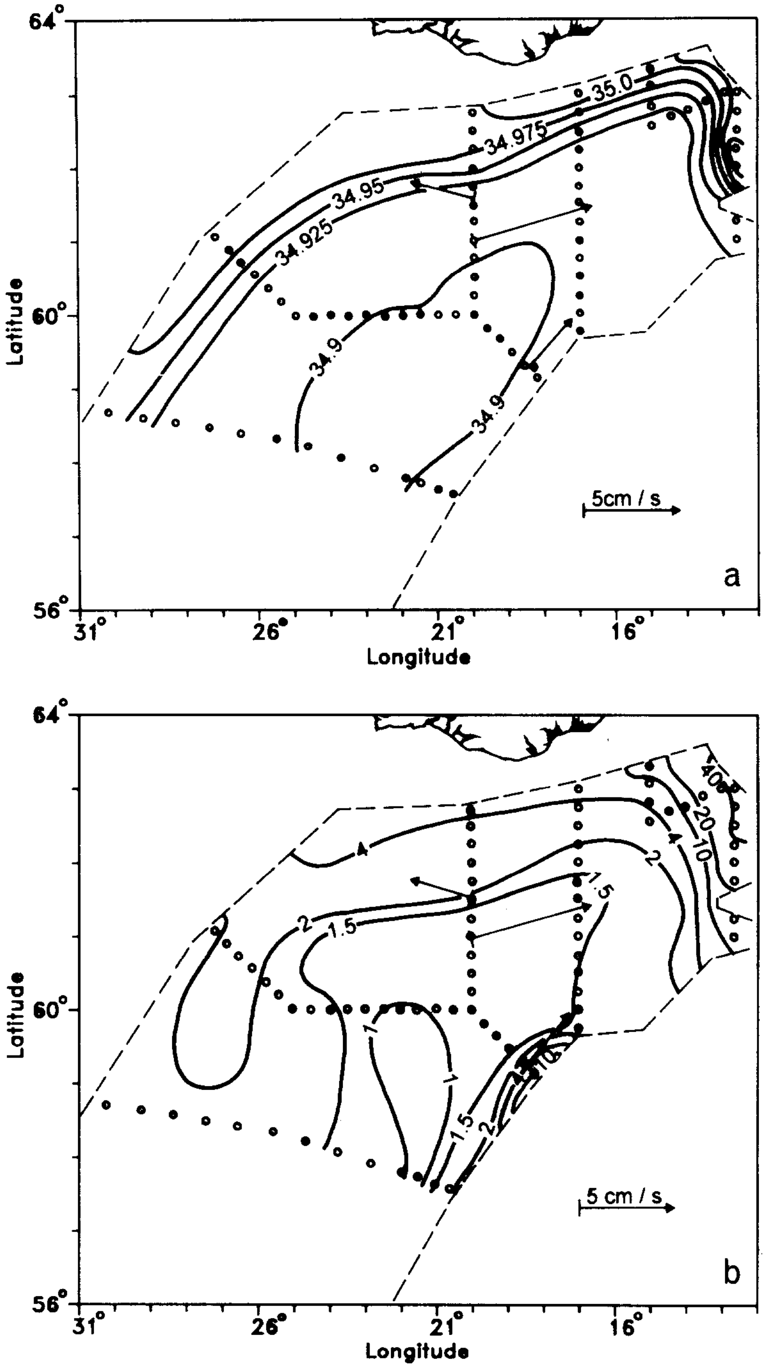

Fig. 9. Isopycnal distribution of (a) S and (b) λ ($\times 10^{11}$ m^{-1} s^{-1}) on the $\sigma_{1.5}$ = 34.64 kg m^{-3} surface for the 1991 survey. This density surface is typical for the LSW core. The current vectors for the closest current meters from moorings IB90/1, IB90/2 and IB90/3 within 200 m from the density surfaces have been drawn. The dashed line indicates the estimated grounding line of the density surface.

mean flow is directed eastwards with a velocity of 6.2 cm s^{-1}. Near 61°35′N, 20°W (IB89/1, IB90/1) at a depth of 1520 m, south of the thermohaline front between the LSW core and the slope water mass, a long-term westward flow of the order of 3.1 cm s^{-1} was observed. The horizontal resolution of the current measurements does not allow a quantitative estimate of the transport of LSW through the Iceland Basin. But the mean currents described above support TALLEY and MCCARTNEY (1982) and TSUCHIYA *et al.* (1992), who concluded from distributions of density and tracers that the circulation of LSW within the Iceland Basin is cyclonic, with a westward flow near the Icelandic slope.

3.5. *Lower Deep Water*

MCCARTNEY (1992) states that LDW in the eastern North Atlantic, which contains a relatively large amount of Antarctic Bottom Water (AABW), contributes considerably to the Deep Northern Boundary Current (DNBC), even before the overflow water from the Norwegian Sea enters the DNBC. In the property–property plots (Fig. 2) we recognize LDW as a high Si and NO_3, low S and O_2, cold water type. LDW is found only in minor amounts in the northern Iceland Basin, since it does not show up as a separate probability maximum in the $P(\Theta, S)$ distribution (Fig. 3). Local characteristic tracer values for LDW in the Maury Channel at 54°N are $\Theta = 2.24$°C, S = 34.94, and Si = 33.0 μmol kg^{-1} (VAN AKEN, 1990). Especially Si appears to be a good tracer for LDW (VAN BENNEKOM, 1985).

Whereas south of the Rockall Bank Si values of about 45 μmol kg^{-1} have been found in the bottom layers below 4000 dbar with $\sigma_{2.5} > 39.30$ kg m^{-3} (VAN AKEN, 1990), the highest Si values in the Maury Channel at 58°N do not exceed 20 μmol kg^{-1} (Fig. 4d) with $\sigma_{2.5} <$ 39.28 kg m^{-3}. This shows that the denser parts of the LDW do not reach the northern Iceland Basin but instead turn south in the deeper parts of the Maury Channel, as proposed by MCCARTNEY (1992). At 58°N LDW can be found above 2400 dbar over the slope of the Hatton Bank as well as in a deep intrusion 100–300 m above the bottom in the Maury Channel (Fig. 4). The slope of the isotherms (which closely follow the isopycnals) clearly indicates that LDW enters the Iceland Basin, advected in a baroclinic DNBC along the Hatton Bank (Fig. 4a), as proposed by MCCARTNEY (1992). In the northern Iceland Basin LDW is observed with Si maxima at 100–300 dbar above the bottom and with maximum values along the Hatton slope (Figs 5d and 6d). Occasionally Si maxima are found near the bottom away from the Hatton slope (e.g. Fig. 6d at 200 km), but in these cases the bottom water is relatively warm, $\Theta > 2.50$°C (Fig. 6a). This suggests that the DNBC follows the Hatton slope well into the northern Iceland Basin and that from the DNBC LDW spreads laterally, often in intrusions overlying the colder overflow waters because of the lower density of LDW. The horizontal distribution of the Si maxima along the hydrographic sections A–F is patchy (Figs 5 and 6), with a typical horizontal length scale of 50–100 km which is hardly resolved with the 28 km station distance. The intrusion level where the Si maxima are found in the northern Iceland Basin is situated close to the $\sigma_{2.5} = 39.245$ kg m^{-3} potential density surface. Plots of Si versus S and λ in this density surface clearly show that the LDW patches with high Si have low S and low λ values (Fig. 10). The observed variations of λ are mainly caused by variations in N and therefore in the vertical spacing of the isopycnals, since the variations in f are only of minor importance. The correlations shown in Fig. 10 indicate that the low S, high Si LDW mainly is found in anticyclonic, baroclinic lenses with large isopycnal spacing, while the competing high S, low Si water is found in cyclonic lenses with small isopycnal spacing.

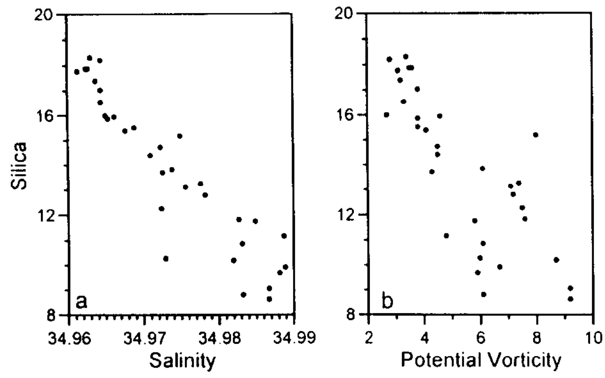

Fig. 10. Plots of Si (μmol kg^{-1}) versus S (a) and versus λ (10^{-11} m^{-1} s^{-1}) (b) on the $\sigma_{2.5}$ = 39.245 kg m^{-3} surface for the stations of sections A–F from 1991 where an Si maximum above the near bottom ISOW layer was observed. This density surface is typical for the LDW intrusions in the northern Iceland Basin.

3.6. *Iceland Scotland Overflow Water*

During the overflow of Norwegian Sea Deep Water (NSDW) and different types of Arctic Intermediate Water (AI) across the sills in the Faroe Bank Channel and over the Iceland–Faroe Ridge (van Aken and Eisma, 1987), these water types mix with each other and entrain overlying SPMW. Hereby a new more or less homogeneous water type, ISOW, is formed (Ellett and Martin, 1973; Harvey and Theodorou, 1986, their ISOW1; McCartney, 1992). Near the Iceland–Faroe Ridge ISOW was encountered only at two neighbouring stations at section I. At Sta. 128 near bottom water with $\Theta \approx 2.00$°C was observed (Fig. 11a), while at Sta. 127 the near bottom water was 0.60°C warmer (Fig. 11b). At Sta. 121 of section H the presence of a cold low salinity intrusion (S < 34.90, $\Theta <$ 2.70°C) above the overflow core near the bottom reflects the contribution of low salinity upper AI of polar origin to the overflow and formation of ISOW. West of section H the different water types contributing to the formation of ISOW appear to be mixed sufficiently to consider ISOW as a single water type. In Fig. 2 ISOW can be recognized as a water type with low temperatures and nutrient concentrations, but with relatively high salinities and O_2 concentrations. The salinity of ISOW reported here is lower than the salinities in the ISOW core reported by Harvey and Theodorou (1986) from a compilation of historic data. They found S > 35.04 along the Icelandic slope. The distribution of $P(\Theta$, S) (Fig. 3) shows only slight changes in the frequency of Θ–S properties of ISOW between 1990 and 1991. From extrapolation of the Si–S and Si–Θ mixing lines the characteristic source water types for ISOW are estimated to be $\Theta \approx 1.75$°C, S $\approx$ 35.00 and Si $\approx$ 7.5 μmol kg^{-1}. These Θ–S properties agree with the properties of ISOW1, reported by Harvey and Theodorou (1986). Given a typical temperature of the overflow of 0.00°C (van Aken and Eisma, 1987), ISOW may already contain 22% entrained SPMW of 8.00°C. This indicates the importance of "warm entrainment" (McCartney, 1992) in the first stages of ISOW formation.

In the central Iceland Basin at 58°N ISOW is found over the Reykjanes Ridge and below the LDW intrusion in the Maury Channel (Fig. 4). In the northern Iceland Basin the cold, high S and O_2 and low Si water is found in a thin, deep bottom layer, often below intrusions

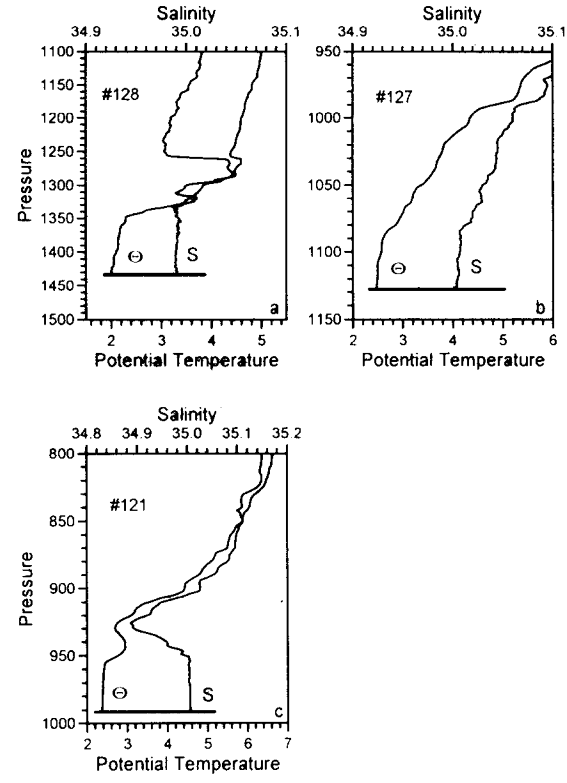

Fig. 11. Profiles of Θ and S for the stations near the Iceland Faroe Ridge where the ISOW core has been observed: Sta. 128 of section I with the coldest water observed in 1991 (a); the neighbouring Sta. 127 (b); and Sta. 121 of section H, where a cold, fresh intrusion overlies the near bottom cold core (c).

of LDW characterized by low O_2 and high Si values (Figs 5 and 6). The slope of the isotherms, and therefore of the isopycnals, in the deep bottom layers closely follows the topography over the Icelandic and Reykjanes slopes (Figs 4a, 5a and 6a). This indicates a baroclinic flow of ISOW, steered by the topography, advecting ISOW in a cyclonic way along these slopes. Above the ISOW layer at section F a conspicuous feature is observed, where the 3.5°C isotherm (Fig. 6a) indicates the presence of relatively warm water in between the cold water in the bottom layer and the overlying LSW. The Si concentration in this warm but stable intrusion appears to be a relative minimum of about 10.7 μmol kg^{-1}.

The potential density level $\sigma_{2.5} = 39.30$ kg m^{-3} is situated about 100 m above the bottom in the deep Iceland Basin, below the level where the Si maxima and O_2 minima related to LDW are observed. This density level is typical for the upper part of the ISOW layer. In this density surface S is well correlated with Si (Fig. 12) with the exception of sections H and I (thick dots). This implies that the modification of ISOW in the deep Iceland Basin can be considered as due to two-component mixing (ISOW with the overlying LDW), the "cold entrainment" proposed by McCartney (1992). Close to the Faroe–Iceland Ridge more components (probably at least NSDW, upper AI and SPMW) all with low Si but with varying S are involved in the formation of ISOW. The close linear relation between S and

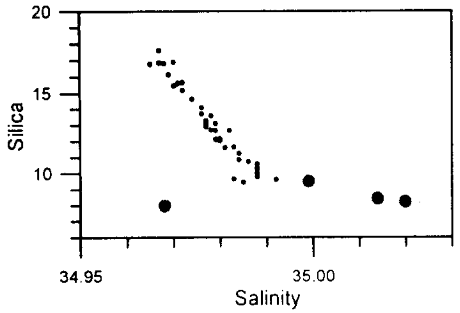

Fig. 12. Si (μmol kg^{-1})–S plot for points in the $\sigma_{2.5}$ = 39.30 kg m^{-3} surface for all stations in the Iceland Basin from the 1991 survey. This density surface is characteristic for ISOW. The thick dots represent the stations on sections H and I.

Si for sections AR7 and A–G does not show any evidence of regeneration of Si for the time scale of the flushing of the deep Iceland Basin.

The lateral distribution of Si in the $\sigma_{2.5}$ = 39.30 kg m^{-3} surface (Fig. 13) shows a low Si core entering the Iceland Basin along the Iceland–Faroe Ridge in a vein that is narrow compared to the width of the slope. This core spreads along the Icelandic and Reykjanes slopes, while high Si values are concentrated along the edge of the Hatton Bank. Downstream of the Iceland–Faroe Ridge the mean Si value across the Iceland Basin decreases monotonically. Mean current vectors observed at 40 m from the bottom (Table 2) are shown in Fig. 13. Near 61°35′N, 20°W current measurements show a steady

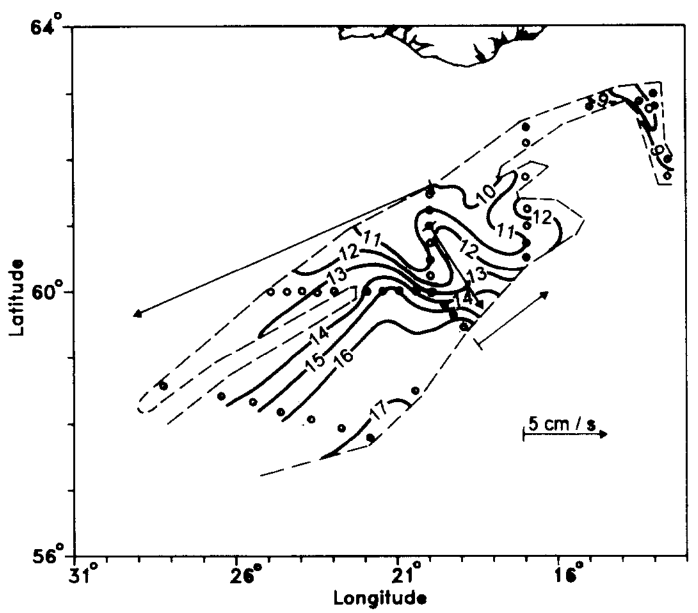

Fig. 13. Isopycnal distribution of Si (μmol kg^{-1}) in the $\sigma_{2.5}$ = 39.3 kg m^{-3} surface for the 1991 survey. This density surface is characteristic for ISOW. The mean current vectors from the current meters at 40 m from the bottom are shown. The dashed line indicates the estimated grounding line of the surface.

westward flow in the lowest 200 m of the order of 13–19 cm s^{-1} (Table 2, IB89/1, IB90/1). At only 35 n. miles more to the south the near bottom velocity is directed south-eastwards with a magnitude of over 5 cm s^{-1} (Table 2, IB90/2). This change of direction is probably due to topographic effects. A small ridge on the Icelandic slope extending from the West Katla Ridge (Shor *et al.*, 1977) is oriented NW–SE and just passes along 60°N, 20°W. This Ridge probably causes the lateral veering of the current direction as was also observed near the East Katla Ridge (Shor *et al.*, 1977). The lateral Si distribution within the ISOW (Fig. 13) shows southward extensions near 20°W and 18°W, probably caused by the topographic loops of the ISOW flow around both Katla Ridges. Along the Hatton slope high Si water appears to flow north–eastwards with a velocity of the order of 5 cm s^{-1} (Table 2, IB90/3).

The mean distance from the $\sigma_{2.5} = 39.30$ kg m^{-3} surface to the bottom amounts to 70 dbar, with a slight tendency to decrease from section F (78 dbar) to section B (59 dbar). This density surface was encountered on only a single station of the 1990 AR7 section in the Iceland Basin. The mean salinity in this surface has, in coherence with Si (Fig. 12), a tendency to decrease by about 0.003 from F to B further downstream. Whereas the downstream thinning of the lowest ISOW layer can be ascribed to divergence of the velocity, the downstream increase of Si and decrease of S suggest that the main cause of the decrease of the mass below the $\sigma_{2.5} = 39.30$ kg m^{-3} surface is due to the decrease of the density of the bottom layer caused by mixing with overlying water (LDW) with lower density.

3.7. *Icelandic Slope Water*

From the vertical tracer sections (Figs 4–6) as well as from the isopycnal tracer distributions (Figs 9 and 13) discussed above, it has become clear that over the Icelandic and Reykjanes slopes a water mass is encountered at intermediate and deep water levels which is characterized by high S and O_2 values and low nutrient values compared with the water mass at the same depth levels in the centre of the Iceland Basin. Tentatively we will call this water mass Icelandic Slope Water (ISW). The frequent occurrence of this water mass can also be seen on the isolated secondary maximum of $P(\Theta, S)$ near $\Theta = 4$°C, S = 34.97–34.99. ISW appears to originate from the region near the Iceland–Faroe Ridge. The property–property plots (Fig. 2) suggest that ISW is mainly a mixture of SPMW and ISOW with some additional LSW in varying mixing ratios. At the ISOW level ISW represents the purest form of ISOW.

3.8. *Quantitative water mass analysis*

Another way to present the hydrographic data is by means of a quantitative water mass analysis, which in effect is a linear transformation of the original hydrographic data. Here we will use the quantitative water mass analysis to clarify processes modifying ISOW in the Iceland Basin. Therefore we will assume that a homogeneous source water type ISOW is formed during the overflow process. After passing the overflow sills ISOW first interacts directly with the overlying SPMW and when descending into the deep Iceland Basin ISOW may mix with LSW, while in the deep basin mixing with LDW may also occur. The ISW water mass is also assumed to be formed in this way. Any influence of the bio-geochemically defined IW on the modification of ISOW will be ignored since this water

Table 3. *Characteristic parameters for the source water types used for the quantitative water mass analysis in section* 3.8

Water type	Θ (°C)	S	Si (μmol kg^{-1})
SPMW	8.00	35.23	6.3
LSW	3.40	34.885	10.5
LDW	2.42	34.94	33.0
ISOW	1.75	35.00	7.5

type is hardly found near the shallow overflow sills. For the intermediate layers above the LSW core we will also ignore IW and assume mixing between SPMW, LSW and ISOW, the latter mainly in the ISW water mass. These assumptions imply that for the three-component mixing at levels above the LSW core we only need Θ and S as conservative tracers. At levels below the LSW core a third conservative tracer is needed for which we choose Si, which has the best signal to noise ratio of the available biogeochemical tracers in this depth interval.

The choice of characteristic parameters for the source water types involved is made in a local context. These parameters have to be characteristic for the deep water in the Iceland Basin, not for the possibly distant areas where these water types are originally formed. Such a local definition of water-type parameters will reduce the effects of possible non-conservative behaviour of Si, due to fluxes from the sediment, on the calculations because it reduces the time scale to the flushing time of the Iceland Basin. The Θ–S diagram (Fig. 2a) does not show a single Θ–S relationship for SPMW, but since the SPMW involved in the flushing of intermediate and deep layers appears to originate near the Iceland–Faroe Ridge, we choose the relations as observed near that area and mentioned in the preceding sections. This choice will make the estimates for the SPMW content above the LSW core inaccurate, since there mixing will occur directly with the overlying form of SPMW. For the choice of the ISOW characteristics we do not simply use the parameters as observed near the overflow sites at sections H and I, since there the Polar and Arctic water types are not yet homogenized to a single ISOW water type (see, e.g. Fig. 12). Instead we take the parameters as obtained from extrapolation of the Si–S and Si–Θ mixing lines to the lowest Si values observed at section I. The characteristic source water type parameters are listed in Table 3.

The quantitative water mass analysis is an idealized model, based on the assumption of the existence of completely homogeneous source water types and the conservation equations for observed conservative properties $P_j = (j = 1 - N)$ from a sample and for mass when $N + 1$ source water types with percentage contributions or mass fractions $m_i(i = 0 - N)$ mix completely;

$$\sum_{i=0}^{N} m_i P_{ij} = P_j. \quad \text{with } m_i > 0 \tag{2}$$

$$\sum_{i=0}^{N} m_i = 100, \tag{3}$$

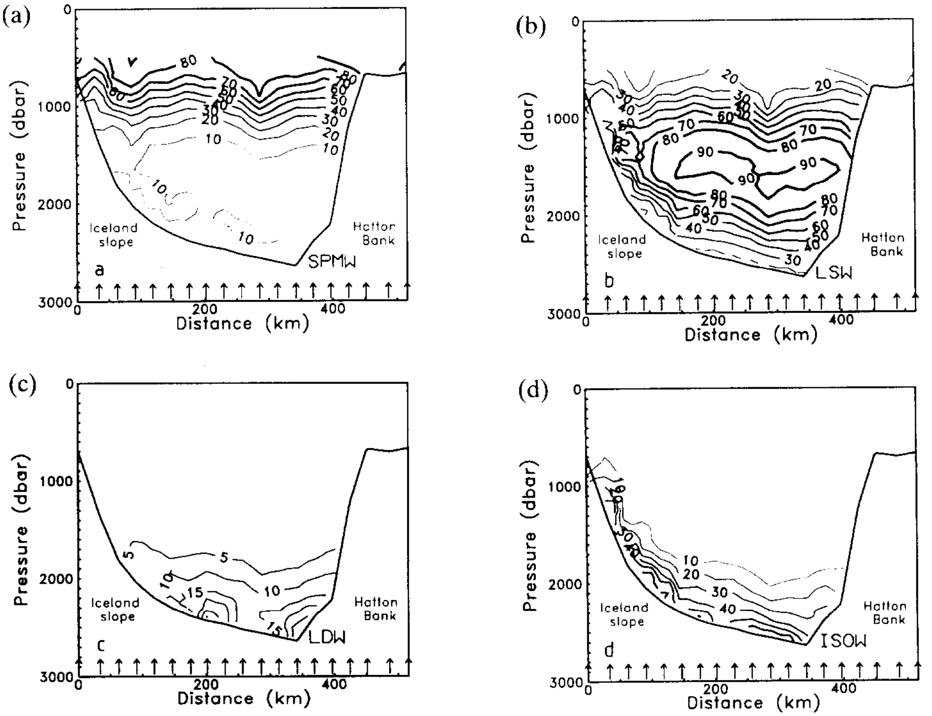

Fig. 14. Vertical sections of mass fractions (%) of SPMW (a), LSW (b), LDW (c) and ISOW (d) along the 1991 zonal section at 17°W. Only the values below 500 dbar have been used.

where m_i is the mass fraction in % and P_{ij} is the value of tracer j for source water type i. It is clear from (2) and (3) that the resulting values of m_i completely depend on the assumptions of the end member properties P_{ij}.

Equations (2) and (3) have been solved for the bottle data, obtained below 500 dbar, according to the conditions stated above. The constraint $m_i > 0$ is maintained by shifting the salinity along Θ levels to the nearest mixing line when initially any $m_i < 0$. This shifting was only needed for the warmest part of the water column above the LSW levels, due to the actual variance of SPMW properties. To identify the mass fraction, we will use the name of the source water type as subscript, e.g. m_{SPMW}. The vertical distribution along section F of the mass fractions of the different water types obtained in this way is shown in Fig. 14.

Figure 14 mainly confirms what already was derived from the original hydrographic parameters. The SPMW at 500 m varies from 70% over the Icelandic slope up to 100% near the Hatton Bank. This is probably due to the real variation in SPMW properties, while we have used the simplification of a single homogeneous source water type. This implies that, above the level of the ISOW core, the quantitative values of m_{SPMW} should be considered with care.

Over the Icelandic slope large amounts of ISOW are found near the bottom (>45% between 1330 and 1500 m) mixed with about 15% SPMW and 35% LSW while in the centre of the Iceland Basin the LSW mass fraction has values of over 90% in the same depth interval (Fig. 14). This result confirms that ISW over the Icelandic shelf indeed is

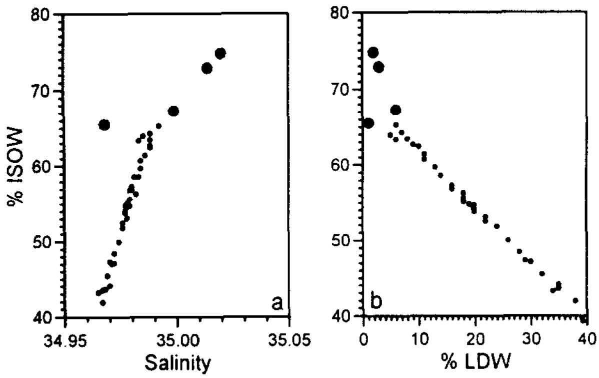

Fig. 15. Plot of the mass fraction of ISOW (%) versus S (a) and versus the mass fraction of LDW (%) (b) in the $\sigma_{2.5} = 39.30\ \mathrm{kg\ m^{-3}}$ surface for all stations from the 1991 survey. This density surface is characteristic for ISOW. The thick dots represent the stations on sections H and I.

formed by mixing in variable amounts of ISOW and SPMW while LSW enters into this water mass laterally by isopycnal mixing. Probably ISW is formed over the Iceland–Faroe Ridge, shortly after passing the overflow sills, by mixing of overflowing cold waters from the Norwegian Sea with the layer of warm and salty Atlantic water (SPMW) which can be found there directly above the ISOW layer. Further down-stream along the Icelandic and Reykjanes slopes ISW is modified further by isopycnal mixing with the water mass from the central Iceland Basin. By the formation of ISW considerable amounts of ISOW are brought to shallow density levels, while in the same process SPMW is removed from the surface layer, recirculating at intermediate and deep levels over the slopes of the Iceland Basin. This indicates the importance of "warm entrainment" (McCartney, 1992) for the formation of ISW.

The SPMW intrusion at section F ($m_{SPMW} > 10\%$) at about 260 dbar from the bottom (Fig. 14a) appears to coincide with the warm intrusion (Fig. 6a) but has a larger southward extension. In this maximum the mean mass fractions are $m_{ISOW} = 36\%$, $m_{SPMW} = 13\%$, $m_{LSW} = 41\%$ and $m_{LDW} = 10\%$. The presence of the m_{SPMW} maximum confirms the hypothesis of van Aken and Eisma (1987) that the vertical stratification in the overflow layer is due to the SPMW content, generated by entrainment during overflow at the sills, with higher amounts of SPMW in the upper parts of the overflow. This is a second process by which SPMW recirculates at deep levels in the Iceland Basin.

The m_{LDW} distribution (Fig. 14c) compares well with the distribution of Si and shows a near bottom inflow of LDW along the Hatton slope and a recirculation over the lower Icelandic slope. The inflow along the Hatton slope of high Si water between 2000 and 2500 dbar at 58°N contained 30–40% LDW, while at section F m_{LDW} values of 25–30% were encountered at the foot of the Hatton slope. The effect of mixing with the fresher LDW on the modification of ISOW, already deduced from Fig. 12, can also be seen from plots of S and m_{LDW} versus m_{ISOW} in the $\sigma_{2.5} = 39.30\ \mathrm{kg\ m^{-3}}$ surface (Fig. 15). These plots also show that near the Iceland–Faroe Ridge (sections H and I) the concept of a single ISOW source water type breaks down because here the formation of ISOW from the original Arctic and Polar water types has not been completed yet.

The modification of ISOW, while flowing downstream from the overflow sills, can be summarized in a histogram showing the ratios of the section averaged mass fractions

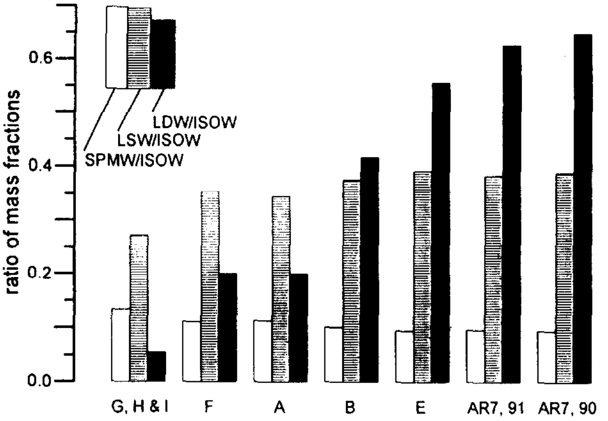

Fig. 16. Histogram of the ratio of the mass fractions m_i/m_{ISOW} for SPMW, LSW and LDW, in the $\sigma_{2.5} = 39.30$ kg m^{-3} surface, averaged over successive sections from the 1991 survey and for section AR7 from the 1990 survey.

m_{SPMW}, m_{LSW} and m_{LDW} divided by m_{ISOW} at the $\sigma_{2.5} = 39.30$ kg m^{-3} surface (Fig. 16). In this density surface, embedded in the near bottom ISOW layer, m_{ISOW} decreased from ≈70% near the Iceland–Faroe Ridge to less than 50% at section AR7, while m_{LDW} increased from less than 5% to over 30%. This is reflected by a continuous increase of the m_{LDW}/m_{ISOW} ratio (Fig. 16). However the ratios m_{SPMW}/m_{ISOW} and m_{LSW}/m_{ISOW} hardly changed between section F and section AR7 (1990), confirming that the modification of ISOW in the deep Iceland Basin mainly occurs by mixing with LDW.

4. DISCUSSION AND CONCLUSIONS

The structure of the distribution of the hydrographic parameters in the Iceland Basin presented above agrees on the basin scale with the structure from the non-synoptic compilations presented by, e.g. TALLEY and MCCARTNEY (1982), HARVEY and THEODOROU (1986) and MCCARTNEY (1992). However, comparisons of these compilations with our data show inter-annual differences. LSW in the Iceland Basin in 1990–1991 had a definitely lower S (0.03–0.05) than in the late fifties and early sixties (TALLEY and MCCARTNEY, 1982), while ISOW in 1990–1991 was fresher (0.05) along the Icelandic slope than shown by HARVEY and THEODOROU (1986) for a compilation of hydrographic data collected between 1955 and 1975. The properties of the water mass over the Icelandic slope, named here ISW, agree with those, observed in 1957–1957 by FUGLISTER (1960), in 1965–1967 by GRANT (1968) and in 1988 by TSUCHIYA *et al.* (1992), compiled by MCCARTNEY (1992). Since the spacing of stations and sections presented here is considerably closer than in most compilations, more detail is shown in our data, like the structure of the deep boundary current along the Hatton Bank (e.g. Fig. 4) and the topographically induced loop of ISOW (Fig. 13). However, no trace of recirculating plumes of ISOW, as shown by HARVEY and THEODOROU (1986), were observed. Possibly these plumes were an artefact, caused by aliasing of temporal, inter-annual changes of ISOW properties to the spatial domain due to the undiscriminating use of data from a 20 year time span in a single data compilation.

The LSW core in its most extreme form (S < 34.90) was observed in the central Iceland Basin (Figs 4–6 and 14b). The regional differences in hydrographic properties of LSW between the Irminger Sea, the Iceland Basin and the Rockall Trough are attributed to differences in the effects of diapycnal mixing while LSW is advected to these basins, although advection of temporal variations of the LSW properties in the Labrador Sea may to some unknown degree contribute to the observed regional differences (READ and GOULD, 1992). Indications of diapycnal mixing of LSW in a boundary current over the Hatton slope have been found (Fig. 9). The isopycnal analysis of LSW as well as current measurements indicate that the main inflow of LSW into the northern Iceland Basin occurs at some distance from the Hatton Bank, with a westward outflow over the Icelandic slope. The resulting cyclonic circulation of LSW was already proposed by TSUCHIYA *et al.* (1992). At the density level of the LSW core, strongly deviating hydrographic properties are observed along the Icelandic and Reykjanes slopes (Fig. 9). Whereas TALLEY and MCCARTNEY (1982) ascribe this to strong diapycnal mixing with ISOW, we assume that here LSW is modified by isopycnal mixing with a slope water mass (ISW) which has its origin near the overflow sills.

From the current observations over the Hatton slope (Table 2) the presence of a branch of the DNBC is deduced which advects LDW along the Hatton Bank into the northern Iceland Basin. This is confirmed by tracer sections which show a narrow baroclinic current with low S and O_2 and high Si along the Hatton slope (Figs 4–6). LDW from this DNBC appears to spread laterally in the form of anticyclonic lenses with low potential vorticity (Fig. 10). From these lenses LDW mixes with the underlying westward flowing ISOW core. With an inflow along the Hatton slope, LDW has a cyclonic circulation on the scale of the Iceland Basin.

The distributions of hydrographic parameters show that the modification of the overflow from the Norwegian Sea occurs in successive stages, as proposed by HARVEY and THEODOROU (1986). Between the sills and 15°W ISOW is formed by mixing of NSDW and AI and entrainment of SPMW (warm entrainment, MCCARTNEY, 1992) and LSW. In the deep Iceland Basin the ISOW core is advected westwards, following the topography in a baroclinic flow, as derived from hydrographic sections (Figs 4–6), isopycnal analyses and current measurements (Fig. 13). There the mutual ratios of the mass fractions of hypothetical ISOW, SPMW and LSW source water types remain constant at the $\sigma_{2.5}$ = 39.30 kg m^{-3} surface, while the contribution of LDW increases from the Iceland–Faroe Ridge westwards (Fig. 16). This confirms that LDW with a strong Si signal recirculates in a cyclonic way in the Iceland basin and mixes with the ISOW core (cold entrainment, MCCARTNEY, 1992). By mixing with LDW the salinity of the ISOW core decreases and its Si content increases (Figs 12 and 15). No indication was found of an increase of the salinity of the ISOW core by mixing with Mediterranean Overflow Water, as proposed by HARVEY and THEODOROU (1986).

In the deep Icelandic Basin amounts of SPMW may be found in the form of a warm intrusion (Fig. 6a) and a m_{SPMW} maximum (Fig. 14a) over the ISOW core at about 260 m above the bottom. This is a residual of "warm entrainment" during the Overflow process (VAN AKEN and EISMA, 1987; MCCARTNEY, 1992). The SPMW maxima are found at about the same density level as the Si maxima, connected to the lenses with LDW. It is probably this relatively warm and salty water with high SPMW content which determines the high salinity, low potential vorticity end member of the regression at the $\sigma_{2.5}$ = 39.245 kg m^{-3} level (Fig. 10).

A water mass (ISW) is observed over the steep Icelandic slope with properties which strongly deviate from the water mass in the central Iceland Basin. The differences are mainly ascribed to reduced amounts of IW, LSW and LDW over the slope (Fig. 14). The origin of ISW is assumed to be near the overflow sills, where SPMW and cold Arctic water types can mix directly, without any other interfering water types (VAN AKEN and EISMA, 1987). The lighter fractions which are formed by this mixing process from the ISW water mass, while the denser fractions are found in the deep ISOW core. The hydrographic sections (Figs 4–6) and isopycnal analysis (Fig. 9) show that at intermediate levels ISW modifies the water mass in the central Iceland Basin by isopycnal mixing with LSW and IW. For the total transports of ISOW and recirculating SPMW (MCCARTNEY and TALLEY, 1984) the contribution of ISW to the budgets should be taken into account.

Summarizing we conclude that the synoptic surveys presented here show that the intermediate and deep water masses in the Iceland Basin are advected in a cyclonic way. In the Iceland Basin they become modified by diapycnal mixing as well as by isopycnal mixing with the water mass over the Icelandic slope which is formed initially by mixing of overflow water with the directly overlying warm SPMW near the sills over the Iceland–Faroe Ridge in the Faroe Bank Channel (warm entrainment). During its descent from the shallow overflow sills, ISOW meets successively SPMW, LSW and LDW. This leads to successive modification stages of ISOW by diapycnal mixing. In the deep Iceland Basin the main modification of ISOW occurs by diapycnal mixing with LDW (cold entrainment).

Acknowledgements—The research reported here was supported by the foundation for Ocean Research (SOZ) and the Working Community for Meteorology and Oceanography (MFO), both of the Netherlands Foundation for Scientific Research (NWO).

We thank the captain and crew of R.V. *Tyro* and the technicians involved in this programme for their kind and skilful co-operation. Special thanks go to S. Ober, R. de Koster, R. Manuels, R. de Vries, K. Bakker, H. Malsschaert and R. Groenewegen who performed analyses and maintained and operated the instrumentation.

REFERENCES

BREWER P. G., W. S. BROECKER, W. S. JENKINS, P. B. RHINES, C. G. ROOTH, J. H. SWIFT, T. TAKAHASHI and R. T. WILLIAMS (1983) A climatic freshening of the deep Atlantic, north of the 50°N over the past 20 years. *Science*, **222**, 1237–1239.

BROECKER W. S. and T. TAKAHASHI (1980) Hydrography of the central Atlantic—III. The North Atlantic deep-water complex. *Deep-Sea Research*, **27**, 591–613.

BROECKER W. S. and T. TAKAHASHI (1981) Hydrography of the central Atlantic.—IV. Intermediate waters of Antarctic origin. *Deep-Sea Research*, **28**, 177–193.

DE BOER C. J. (1993) Water mass distribution in the Iceland Basin calculated with an optical parameter analysis. ICES C.M. 1993/C:16.

DICKSON R. R., E. M. GMITROWICZ and A. J. WATSON (1990) Deep-water renewal in the northern North Atlantic. *Nature*, **344**, 848–850.

DOOLEY H. D. and J. MEINCKE (1981) Circulation and water masses in the Faroese Channels during Overflow '73. *Deutsche Hydrographische Zeitschrift*, **34**, 41–54.

DOOLEY H. D., J. H. A. MARTIN and D. J. ELLETT (1984) Abnormal hydrographic conditions in the north east Atlantic during the 1970s. *Rapport et Procès-verbaux des Réunions Conseil Permanent International pour Exploration de la Mer*, **185**, 179–185.

ELLETT D. J. and J. H. A. MARTIN (1973) The physical and chemical oceanography of the Rockall Channel. *Deep-Sea Research*, **20**, 585–625.

ELLETT D. J. and D. G. ROBERTS (1973) The overflow of Norwegian Sea Deep Water across the Wyville Thomson Ridge. *Deep-Sea Research*, **20**, 819–835.

FUGLISTER F. C. (1960) Atlantic Ocean Atlas of temperature and salinity profiles and data from the International Geophysical Year of 1957–1958. Woods Hole Oceanographic Institution Atlas Series, **1**, 209 pp.

GRANT A. B. (1968) Atlas of oceanographic sections: Temperature–salinity–dissolved oxygen–silica. Davis

Strait–Labrador Basin–Denmark Strait–Newfoundland Basin, 1965–1967. *Atlantic Oceanographic Laboratory*, Rep. A.O.L.68-5, Bedford Institute of Oceanography, Dartmouth, N.S., Canada.

HARVEY J. G. and A. THEODOROU (1986) The circulation of Norwegian Sea overflow water in the eastern North Atlantic. *Oceanologica Acta*, **9**, 393–402.

JPOTS editorial panel (1991) Processing of oceanographic station data. UNESCO, Paris, 138 pp.

KAWASE M. and J. L. SARMIENTO (1986) Circulation and nutrients in mid depth Atlantic waters. *Journal of Geophysical Research*, **91**, 9749–9770.

LEE A. and D. J. ELLETT (1965) On the contribution of overflow water from the Norwegian sea to the hydrographic structure of the North Atlantic Ocean. *Deep-Sea Research*, **12**, 129–142.

MANN C. R., A. R. COOTE and D. M. GARNER (1973) The meridional distribution of silicate in the western Atlantic Ocean. *Deep-Sea Research*, **20**, 791–801.

MCCARTNEY M. S. (1992) Recirculating components of the deep boundary current of the northern North Atlantic. *Progress in Oceanography*, **29**, 283–383.

MCCARTNEY M. S. and L. D. TALLEY (1982) The Subpolar Mode Water of the North Atlantic Ocean. *Journal of Physical Oceanography*, **12**, 1169–1189.

MCCARTNEY M. S. and L. D. TALLEY (1984) Warm-to-cold water conversion in the Northern Atlantic Ocean. *Journal of Physical Oceanography*, **14**, 922–935.

MCDOWELL S., P. RHINES and T. KEFFER (1982) North Atlantic Potential Vorticity and its relation with general circulation. *Journal of Physical Oceanography*, **12**, 1417–1436.

READ J. F. and W. J. GOULD (1992) Cooling and freshening of the Subpolar North Atlantic Ocean since the 1960s. *Nature*, **360**, 55–57.

RUDELS B. and D. QUADFASEL (1991) The Arctic Ocean component in the Greenland–Scotland overflow. ICES C.M.1991/C:30, 10 pp. + Figs.

SHOR A., D. MULLER and D. JOHNSON (1977) Transport of Norwegian Sea Overflow—preliminary results of Atlantis cruise 94, June–July 1977. ICES C.M. 1977/C:44.

SWIFT J. H. and K. AAGAARD (1981) Seasonal transitions and water mass formation in the Iceland and Greenland Seas. *Deep-Sea Research*, **28**, 1107–1129.

TALLEY L. D. and M. S. MCCARTNEY (1982) Distribution and circulation of Labrador Sea Water. *Journal of Physical Oceanography*, **12**, 1189–1205.

TSUCHIYA M. (1989) Circulation of the Antarctic intermediate Water in the North Atlantic Ocean. *Journal of Marine Research*, **47**, 747–755.

VAN AKEN H. M. (1990) DUTCH-WARP 1990, R.V. *Tyro* cruise 90/3. Part I: WOCE section AR7E. (cruise report) NIOZ, Texel, (17 pp + Figs).

VAN AKEN H. M. (1992) DUTCH-WARP 91, R.V. *Tyro* cruise 91/1, Part 1, WOCE hydrographic Programme, section AR7E (cruise report) NIOZ, Texel (34 pp. + Figs).

VAN AKEN H. M. (1993) Current measurement in the Iceland Basin. ICES C.M. 1993/C:11.

VAN AKEN H. M. and D. EISMA (1987) The circulation between Iceland and Scotland derived from water mass analysis. *Netherlands Journal of Sea Research*, **21**, 1–15.

VAN AKEN H. M. and S. OBER (1991) A compilation of moored current meter data from the Iceland Basin (DUTCH-WARP 89, mooring IB89/1). NIOZ Data Report 1991–2, NIOZ, Texel, 8 pp. + Figs.

VAN AKEN H. M. and S. OBER (1992) A compilation of moored current meter data from the Iceland Basin (DUTCH-WARP 90, moorings IB90/1,2,3 and 4). NIOZ Data Report 1992–1, NIOZ, Texel, 16 pp. + Figs.

VAN BENNEKOM (1985) Dissolved silica as an indicator of Antarctic Bottom Water penetration and the variability in the bottom layers of the Norwegian and Icelandic Basins. *Rit fiskideildar*, **9**, 101–109.

WORTHINGTON L. V. (1981) The water masses of the World Ocean: some results of a fine scale census. In: *Evolution of physical oceanography*. B. A. WARREN and C. WUNSCH, editors, The MIT Press, pp. 42–69.